Magnetic Signature of Basalts in the Chang'e-5 Sample Region: Implications for the Lunar Dynamo

Teng Hu[1,2,3], Xiaojian Xu[1,2,3], Shuo Yao[2,3,4], Zhizhong Kang[1,2,3*], Xiaoyun Wan[1,2,3], Carolyn H. van der Bogert[5], Harald Hiesinger[5]

[1]School of Land Science and Technology, China University of Geosciences (Beijing), Beijing, China; [2]Research Center of Lunar and Planetary Remote Sensing Exploration, China University of Geosciences (Beijing), Beijing, China; [3]Subcenter of International Cooperation and Research on Lunar and Planetary Exploration, Center of Space Exploration, Ministry of Education of the People's Republic of China, Beijing, China; [4]School of Geophysics and Information Technology, China University of Geosciences (Beijing), Beijing, China; [5]Institut für Planetologie, Westfälische Wilhelms-Universität Münster, Münster, Germany

Key Points:

- Younger lava from Rima Mairan filled the southern region of Em4/P58 and backfilled Rima Sharp.
- Magnetic field and topography analyses indicate that the lava from Rima Mairan was not magnetized compared to lava emplaced to the rest of Em4/P58.
- Thus, analyses of differently-aged basalts at the CE-5 site may help constrain the evolution of the lunar magnetic field over time.

Abstract

In December 2020, Chang'e-5 returned samples from mare basalt unit Em4/P58 in northern Oceanus Procellarum. With an absolute model age of 1.21-1.53 Ga (Hiesinger et al. 2003; Qian et al., 2018, 2021a). Elevation analysis of the interior of Rima Sharp and Mairan, plus geomorphological observations suggest lava backfilling of Rima Sharp with younger lava from Rima Mairan. Analysis of the magnetic field at the surface also shows that the younger lava from the southern Mairan vents, which covered the southeastern part of Em4/P58 is unmagnetized. Our new magnetic anomaly analysis shows that Em4/P58 unit can be divided into magnetized (northwest) and unmagnetized (southeast) parts. The comprehensive analysis of magnetic anomaly and topography shows that lava from southern rille is likely to have reached the Chang'e-5 landing site. Samples returned by Chang'e-5 will help constrain the source of lava flow and the evolution of the lunar magnetic field over time.

Plain Language Summary

The age and nature of the youngest lunar lava flows is an important question in planetary science that remains open. With this in mind, China's Chang'e-5 mission aimed to collect samples from one of the youngest basalts on the Moon.

Investigations of the area covered by the collected basalts and time sequence of the lava flows using remote sensing data aid in understanding the source and nature of the lavas. We analyze the nature and coverage of lava from the three lava vents based on terrain, topographic features, and magnetic field data. The results show that older lava from north and northwest of the landing site is magnetized, whereas younger lava from the south is not magnetized. We also found evidence that the younger lava may cover Chang'e-5 landing site, and was likely sampled. The results of the sample analysis may help us understand the nature and evolution of the lunar magnetic field.

Keywords: Chang'e-5; Landing site; Lava flow; Magnetic Signature.

1 Introduction

The Chang'e-5 sample return site is located in northern Oceanus Procellarum in an area that has been shown to be 1.33 Ga old dated by Hiesinger et al. (2003) as their P58 unit, ~1.21 Ga by Qian et al. (2018) as their Em4 unit, and ~1.53 Ga by Qian et al. (2021a). The new Chang'e-5 samples will help us to better understand the composition of the mare basalts as well as to further constrain their ages. The young basalts in the so-called Em4/P58 area have attracted a lot of attention, not only because of their young age, but also with respect to their potential lava sources: Zhao et al. (2017) and Qian et al. (2018) considered whether Mons Rümker may be the source of the lava. Since then, Qian et al. (2021a) found that the age of Mons Rümker is different from that of Em4/P58 and suggested that three nearby rilles in Em4/P58 are the lava sources.

In order to better understand the evolution of the landing site region and the characteristics of lava ascent and eruption from the late Eratosthenian to the Copernican, this study uses multiple data sources for stratigraphic analyses (e.g., superposition) as well as identification of the lava sources of Em4/P58. This study aims to understand the characteristics of magmatic eruptions, lunar surface magnetization as well as the geological history and evolution of northern Oceanus Procellarum from the late Eratosthenian to the Copernican.

2 Research Area & Data

2.1 Description of the Research Area

The Em4/P58 basalt unit (Hiesinger et al., 2003) has an area of 33931 km^2, and is located in the northern Oceanus Procellarum, to the east of Mons Rümker and west of Mons Jura on the northwestern edge of Mare Imbrium. Crater size-frequency distribution (CSFD) measurements indicate that the mare basalts in this area were formed 1.3 Ga ago making Em4/P58 one of the youngest geological units on the Moon (Qian et al., 2018; Hiesinger et al., 2011). A large-scale wrinkle ridge system occurs in the western part of Em4/P58, and what was originally thought to be the longest rille on the Moon – Rima Sharp (Hurwitz

et al., 2013) is found in the eastern plain. Recently, Qian et al. (2021c) showed that this rille is a compound system of four rilles, where Rima Sharp and Rima Mairan actually meet in the eastern plain to form a long system. In the CE-5 landing region, the Em4/P58 unit exhibits moderate-Ti (5-8 wt.%), high-Th content (5-8.5 ppm), and relatively high-olivine Eratosthenian-aged mare basalts (~13 wt.%) (Qian et al., 2021c). According to Lemelin et al. (2015)'s global mineral abundance data, the absolute mineral abundances of clinopyroxene, orthopyroxene, olivine, and plagioclase are 30, 16, 13 and 41 wt.%, respectively (Qian et al. 2021).

2.2 Description of Research Data

The data used in this work include Chang'e-2 CCD stereo camera images from which a digital orthophoto map (DOM) was calculated with a pixel scale of 7 m, in addition to the LRO LROC WAC Global Morphology Mosaic (100 m/pixel) (Speyerer et al., 2011). To study the topography of the Em4/P58 study area, we used SLDEM2015 data (60m/pixel, Barker et al., 2016) and. The magnetic field on the lunar surface is calculated from the magnetic measurements made at altitudes of 10-45 km by Kaguya and Lunar Prospector (Tsunakawa et al. 2015). The spatial resolution of the calculated magnetic field is 0.2 degrees, which is about 6 km/pixel at this location.

3 Methods and Results

3.1 Morphological Analysis

The digital elevation and orthophoto maps (DEM, DOM) were used to interpret the topographic characteristics of structures and rilles in the Em4/P58 unit, and the image data were used determine their geographical distribution and morphological characteristics. The goal of this part of the study was to identify and evaluate structural and morphological evidence for the magmatic activity in this region. Using the orthomosaic, we digitized three rilles with a total length of 587 km which occur both in the interior and along the edge of Em4/P58. These are largely the same as those described by Qian et al. (2020). In order to determine the scale of lava spreading through rilles, we used the DEM data to derive elevation profiles across the wrinkle ridges and along the rilles. In addition, topographic slopes were investigated to determine the flow direction and extent of lava flow. Our high-resolution DOM shows the texture and structure of the rilles, which can help us to better understand their formation.

Terrain analysis The DEM of Em4/P58 unit is shown in Figure 1(a). The elevation in the region is between -2400m and -2700m, decreasing by 50-100 m from west to east. The topographic variability in the study area is mainly related to the wrinkle ridges, which can be 200 m higher than the surrounding regional basalt plains. The largest wrinkle ridges system is located in the western part of Em4/P58. Both Rima Sharp (from the northern vents) and Rima Mairan

(from the southern vents) traverse the deepest part of Em4/P58, meet in the eastern central part of Em4/P58 (see also Qian et al., 2021c).

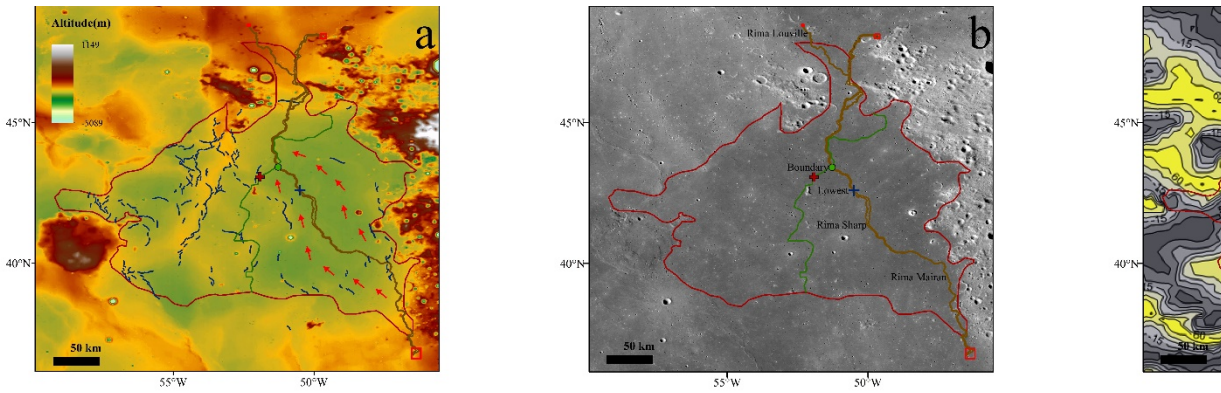

Figure 1. Red line: outline of P58, blue lines: wrinkle ridges, brown lines: rilles, green line: boundary of high and low magnatic field, red cross: Chang'e-5 landing site, red square: lava source vents. (a) DEM of Em4/P58 unit. (b) Digital orthophoto map. (c) Magnetic field inclination on P58 surface. (d) Crustal magnetic field of P58 and lava boundary. (e) and (f) Evidence of lava backfill from ground to Rima Sharp at 43°31'N, 51°18W (Figure 1e), and 43°22'N, 51°17'W (Figure 1f), where close to the magnatic boundary. (g) Rima Sharp/Mairan elevation profile.

Geomorphologic and topographic analysis Detailed observations of the rilles in the study area led Qian et al. (2021c) to conclude that lavas delivered by Rima Sharp were sourced from northern vents, whereas additional lava was delivered via Rima Mairan from the south. LROC NAC images show inner, narrower rilles within Rima Sharp (e.g., Qian et al., 2021c), which indicates that lava from southern vents backfilled Rima Sharp after it formed. We find some gaps in the levees of Rima Sharp (Figure 1e and 1f) where close to the green point in Figure 1a-d. Compared with other parts of the levees, these gaps have a smoother surface (few rocks). Some small gaps are triangle-shaped, retain the traces of lava fanned in Rima Sharp. The terrain characteristics and the existence of the gaps shows that lava from southern vents flow in the southeast part of Em4/P58 to the boundary (Figure 1(a)) and backfilled into

Rima Sharp.

3.2 Magnetic Anomaly Analysis

Three-dimensional amplitude and directional magnetic anomaly inversion are adopted to reveal the distribution of magnetic rocks in the crust under the Chang'e-5 landing site (Li, 2010; Li and Oldenburg, 1996, 2003). The input for the amplitude inversion technique is the amplitude of the magnetic field on the surface, and the output is the 3D distribution of the remanent magnetization subsurface. The input for directional inversion includes the magnetic anomaly along the ancient magnetic field, which is used to simulate the acquisition of magnetization. Here, assumptions must be made for the direction and intensity of the ancient magnetic field. The result of the directional inversion is the apparent magnetic susceptibility that reflects magnetic differences of rocks (Li and Oldenburg, 1996, 2003). The inversion algorithm is given as:

$$S(m) = (B_t - F(m))^T D^{-1} (B_t - F(m)) + (m - m_0)^T W^{-1} (m - m_0)$$

with S being the total objective function for the inversion. The first term on the right is the objective function from data fitting, and the second term is the objective function of the underground model. The dimension of magnitude of the magnetic field Bt is N. The model is represented by m, which includes M units. F represents the nonlinear forward operator. D is a diagonal covariance matrix of the data. The variances of noises are on the diagonal. The initial reference model is m_0, and W is a diagonal covariance matrix of the model underground in the inversion.

The three-dimensional directional inversion divides the source region underground for inversion of the magnetic rock into a series of units (a unit is a cube in the source region), assuming that the apparent magnetic susceptibility in each unit is constant, that is, $d = G_\kappa$.(Li and Oldenburg, 1996, 2003)

In the equation, d is the data vector. In addition, represents the susceptibility vectors in the cells. The matrix G has elements g_{ij} that quantify the contribution of a unit susceptibility in the jth cell to the ith datum of the magnetic anomaly. The functions g_{ij} are the projection onto the given direction of the magnetic field. (Li and Oldenburg, 1996, 2003)

A right-handed Cartesian coordinate system is used in the directional inversion algorithm. The x-direction is northward, the y-direction is eastward, the z-direction points downward. The magnetic inclination of the surface magnetic anomaly (Tsunakawa et al., 2015) is shown in the following Figure 1(c).

The magnetic inclination of the landing site is about 40 degrees. The projection of the magnetic anomaly dB along the possible direction of the ancient magnetic field is dT. Assuming that the magnetic declination is zero, the dT is obtained from the Br (radial outward) and Btheta (north component) in the diagram.

The intensity of the magnetic field of the lunar dynamo is set to be 50000 nT. According to the paleomagnetic field studies of the Moon, the intensity of the ancient dynamo field could be from 100 nT to 100000 nT. It was about 50000 nT 3.2 billion years ago. In this inversion, only the induction magnetization process is considered in order to simulate the magnetization process during the geological history of the Moon (for example what happened at 3 Ga). The magnetization is uniform in each unit of the source region in the inversion and is obtained from the apparent magnetic susceptibility and the external field H.

The lunar magnetic field at the surface calculated from measurement at orbit (Tsunakawa et al. 2015) in the Em4/P58 region is shown in Figure 1(d). From the magnetic field intensity map, it can be seen that the strongest lunar surface magnetic field occurs mainly in the northwestern parts of the study area. The total intensity of the surface magnetic field in most southeastern parts is less than 0.5 nT, which can be interpreted, to a first order, as an absence of a significant surface magnetization. The topographic gaps shown in Fig 1e and 1f also indicated that, the lava from the southern vents covered the southeastern parts, reached the boundary and flowed into Rima Sharp through the gaps in the levees. The absence of magnetization in young magmatic rocks, like those in Em4/P58, is consistent with work that shows that the lunar magnetic field severely decreased about 3 Ga ago (Tikoo et al., 2017; Weiss and Tikoo, 2014; Wang et al., 2017).

4. Lava Source Analysis

4.1 Magnetic Rock Distribution

Basalts in the southeast of unit Em4/P58 are not magnetized. Thus, magnetized magmatic rocks likely never formed in the southeastern parts of the study area. Figure 1d shows evidence for magnetic fields at the magmatic vents in the north and northwest might imply residual lava chambers. However, the rocks at the magmatic vents in the south are not magnetic, indicating that the early eruption of magnetic lava may have originated from the residual volcanic dome in the northwest. If correct, this lava did not reach the southeastern part of unit Em4/P58. As a result, the boundary of lava from north and south can be defined based the magnetic field characteristics (Figure 1(d)).

4.2 Main Lava Sources of Em4/P58 Geological Unit

The lava erupted by the northern vents travelled south through the Rima Sharp. The elevation analysis of Rima Sharp shows that lava erupted by the northern vents does not flow to the south, only to the east of the landing site (across the lowest point and fill the valley bottom of Rima Sharp). The geological evidence of lava backfilling (Figure 1e and 1f) found in Rima Sharp and the elevation analysis of the interior of Rima Sharp show that lava erupted by the southern vents flowed northward and converged with the earlier lava from the north at the lowest point of Rima Sharp. As the lava go north, it spread to the east and

west, covering a large area in the southeast and east of Em4/P58. Hence, on the basis of our analysis, the lava from the southern vents appear to be the main source of basalts in this area.

4.3 Lava Source of Chang'e-5 Landing Site

Located at the topographic inflection point of the surrounding terrain, the Chang'e-5 landing area is higher in elevation in the west compared to the east. Topographically, lava from the northwest will be blocked by wrinkle ridges although the north of the landing area is flat and low-lying. Basalts on the surface are more likely to come from lava from the south or northern vents. According to CSFD results within the Em4/P58 unit, the young basalts in the south were formed at 1.3 Ga (Hiesinger et al., 2003), i.e., at times when an active lunar magnetic field already ceased. Hence, we propose that the shallow non-magnetized basalts in the Chang'e-5 landing area may come from southern sources. In addition, the lava backfill in the east of the landing site (near the lowest point of Rima Sharp) also suggests that the lava of the landing site likely came from the southern vents. The analyses of the rock samples brought back by Chang'e-5 will provide conclusive evidence for the lava source in this area.

On the basis of our magnetic and morphological analyses, we propose that before about 1.0 Ga (Qian et al., 2021a), there were many eruptions in the general Em4/P58 region (northwest, north and south). Lava from the northwest covered a small area, lava from the north spread to the east of the Chang'e-5 landing area through Rima Sharp, and lava from the south was widely distributed and constitutes the main source of the shallow layer of Em4/P58 unit. According to the topographic characteristics, lava from the southern vent spread to the east of the Chang'e-5 landing area and is the most likely source of lava in the Chang'e-5 landing area.

5 Conclusions

1. In the geological unit (Em4/P58) where Chang'e-5 is located, there are three main sources of lava located in the north, south and northwest. Lava from the northern vents formed Rima Sharp. In addition, lava from southern vents went north filling the southern region of Em4/P58 and backfilled Rima Sharp forming gaps in the levees of Rima Sharp and inner, narrower rilles in its interior. Elevation analysis inside Rima Sharp suggests that the lavas from the south reached as far north as 43°24' N, 51°16'W.

2. The magnetic inversion results are interpreted to show magma chambers and magnetized basalt deposits in the northern and northwestern part of Em4/P58. However, magnetic field results show that the rocks in the south exhibit no remnant magnetism. The absence of magnetism in basalts significantly younger then ~3 Ga supports models that the lunar dynamo weakened significant after this point in time.

3. Lava from the southern vents spread to the southeastern part of Em4/P58 and is the most likely a major source of lava in the Chang'e-5 landing area.
4. The results of sample magnetic analysis and material age analysis of Chang'e-5 will contribute to the study of lunar dynamo history.

Acknowledgements and Data

This work was supported by National Natural Science Foundation of China (Grant Nos. 41872207,41602215), National Key Research and Development project (2019YFE0123300), the Pre-research Project on Civil Aerospace Technologies Funded by China National Space Administration (CNSA) (No. D020204) and the German Aerospace Center (Deutsches Zentrum für Luft- und Raumfahrt) project 50OW2001.

Chang'e-2 DOM data are from https://www.scidb.cn/s/J7773i, LROC NAC data are from https://ode.rsl.wustl.edu/moon/indexProductSearch.aspx, LROC WAC data are from http://wms.lroc.asu.edu/lroc/view_rdr/WAC_GLOBAL, SLDEM2015 data are from https://astrogeology.usgs.gov/search/map/Moon/LRO/LOLA/Lunar_LRO_LOL
The magnetic field data are from http://www.geo.titech.ac.jp/lab/tsunakawa/Kaguya_LMAG.

References

Barker, M. K., Mazarico, E., Neumann, G. A., Zuber, M. T., Haruyama, J., & Smith, D. E. (2016). A new lunar digital elevation model from the Lunar Orbiter Laser Altimeter and SELENE Terrain Camera. *Icarus, 273*, 346-355.

Head, J. W., & Wilson, L. (2017). Generation, ascent and eruption of magma on the Moon: New insights into source depths, magma supply, intrusions and effusive/explosive eruptions (Part 2: Predicted emplacement processes and observations). *Icarus, 283*, 176-223. doi:10.1016/j.icarus.2016.05.031

Hiesinger, H., Head, J. W., Wolf, U., Jaumann, R., & Neukum, G. (2003). Ages and stratigraphy of mare basalts in Oceanus Procellarum, Mare Nubium, Mare Cognitum, and Mare Insularum. *Journal of Geophysical Research-Planets, 108*(E7). doi:Artn 5065. doi:10.1029/2002je001985

Hiesinger, H., Head, J. W., Wolf, U., Jaumann, R., & Neukum, G. (2011). Ages and stratigraphy of lunar mare basalts: A synthesis. In *Recent Advances and Current Research Issues in Lunar Stratigraphy.*

Hurwitz, D. M., Head, J. W., & Hiesinger, H. (2013). Lunar sinuous rilles: Distribution, characteristics, and implications for their origin. *Planetary and Space Science, 79-80*, 1-38. doi:https://doi.org/10.1016/j.pss.2012.10.019

Lemoine, F. G., Goossens, S., Sabaka, T. J., Nicholas, J. B., Mazarico, E., Rowlands, D. D., . . . Zuber, M. T. (2014). GRGM900C: A degree 900 lunar gravity model from GRAIL primary and extended mission data. *Geophys Res Lett, 41*(10), 3382-3389. doi:10.1002/2014GL060027

Li, Y., Lynch, B. J., Welsch, B. T., Stenborg, G. A., Luhmann, J. G., Fisher, G. H., . . . Nightingale, R. W. (2010). Sequential Coronal Mass Ejections from AR8038 in May 1997. *Solar Physics, 264*(1), 149-164. doi:10.1007/s11207-010-9547-y

Li, Y. G., & Oldenburg, D. W. (1996). 3-D inversion of magnetic data. *Geophysics, 61*(2), 394-408. Retrieved from <Go to ISI>://WOS:A1996UA26100009

Li, Y. G., & Oldenburg, D. W. (2003). Fast inversion of large-scale magnetic data using wavelet transforms and a logarithmic barrier method. *Geophysical Journal International, 152*(2), 251-265. doi:DOI 10.1046/j.1365-246X.2003.01766.x

Mighani, S., Wang, H. P., Shuster, D. L., Borlina, C. S., Nichols, C. I. O., & Weiss, B. P. (2020). The end of the lunar dynamo. Science Advances, 6(1). doi:ARTN eaax0883 10.1126/sciadv.aax0883

Qian, Y. Q., Xiao, L., Head, J. W., van der Bogert, C. H., Hiesinger, H., & Wilson, L. (2021a). Young lunar mare basalts in the Chang'e-5 sample return region, northern Oceanus Procellarum. *Earth and Planetary Science Letters, 555*. 10.1016/j.epsl.2020.116702

Qian, Y. Q., Xiao L., Head J. W., and Wilson L. (2021b) The long sinuous rille system in Northern Oceanus Procellarum and its relation to the Chang'e-5 returned samples. *Geophysical Research Letters* 48, e2021GL092663.

Qian, Y. Q. et al. (2021c) China's Chang'e-5 landing site: Geology, stratigraphy, and provenance of materials. *Earth and Planetary Science Letters* 561, 116855.

Qian, Y. Q., Xiao, L., Zhao, S. Y., Zhao, J. N., Huang, J., Flahaut, J., . . . Wang, G. X. (2018). Geology and Scientific Significance of the Rumker Region in Northern Oceanus Procellarum: China's Chang'E-5 Landing Region. *Journal of Geophysical Research-Planets, 123*(6), 1407-1430. doi:10.1029/2018je005595

Scott, D. H., & Eggleton, R. E. (1973). Geologic map of the Rümker quadrangle of the Moon.

Speyerer, E., Robinson, M. S., & Denevi, B. W. (2011). Lunar Reconnaissance Orbiter Camera Global Morphological Map of the Moon. In *42nd Lunar and Planetary Science Conference* (p. 2387).

Stoffler, D., & Ryder, G. (2001). Stratigraphy and isotope ages of lunar geologic units: Chronological standard for the inner solar system. *Space Science Reviews, 96*(1-4), 9-54. doi:Doi 10.1023/A:1011937020193

Tikoo, S. M., Weiss, B. P., Shuster, D. L., Suavet, C., Wang, H. P., & Grove, T. L. (2017). A two-billion-year history for the lunar dynamo. *Science Advances,*

3(8). Retrieved from <Go to ISI>://WOS:000411589900031

Tsunakawa, H., Takahashi, F., Shimizu, H., Shibuya, H., & Matsushima, M. (2015). Surface vector mapping of magnetic anomalies over the Moon using Kaguya and Lunar Prospector observations. *Journal of Geophysical Research-Planets, 120*(6), 1160-1185. Retrieved from <Go to ISI>://WOS:000357951300007

Wang, H., Mighani, S., Weiss, B. P., Shuster, D. L., & Hodges, K. V. (2017). *Lifetime of the Lunar Dynamo Constrained by Young Apollo Returned Breccias 15015 and 15465*. https://ui.adsabs.harvard.edu/abs/2017LPI....48.1439W

Weiss, B. P., & Tikoo, S. M. (2014). The lunar dynamo. *Science, 346*(6214), 1198-+. doi:ARTN 1246753, 10.1126/science.1246753

Wilhelms, D. E., McCauley, J. F., & Aeronautical Chart and Information Center (U.S.) (Cartographer). (1971). Geologic map of the near side of the Moon [1 map]

Wilhelms, D. E., McCauley, J. F., & Trask, N. J. (1987). *The geologic history of the moon*. Washington

Wilson, L., & Head, J. W. (2017). Generation, ascent and eruption of magma on the Moon: New insights into source depths, magma supply, intrusions and effusive/explosive eruptions (Part 1: Theory). *Icarus, 283*, 146-175. doi:10.1016/j.icarus.2015.12.039

Zhao, J. N., Xiao, L., Qiao, L., Glotch, T. D., & Huang, Q. (2017). The Mons Rumker volcanic complex of the Moon: A candidate landing site for the Chang'E-5 mission. Journal of Geophysical Research-Planets, 122(7), 1419-1442. doi:10.1002/2016je005247